DESIGN OPTIMIZATION OF LINEAR TRANSFORMER DRIVER (LTD) STAGE CELL CAPACITORS*

Andrew H. Bushnell[ξ], Byeong-Mun Song, Joel Ennis, Richard Miller[1], Dave Johnson[1], John Maenchen[2]

General Atomics Electronic Systems, Inc., San Diego, CA
[1]Titan Pulsed Sciences Division, San Diego, CA, USA
[2]Sandia National Laboratories, Albuquerque, NM, USA

Abstract

Optimizing the design of Linear Transformer Driver (LTD) stage capacitors is important to achieve a very low inductance and short pulse output in pulsed power generators. The stage consists of many LTD capacitor cells. The LTD performance is dependant on the characteristics of each capacitor. The capacitor construction causes distributed transmission line properties that impact the transfer of energy in terms of efficiency and time.

This paper focuses on the characterization and analysis of Linear Transformer Driver (LTD) cell capacitors in pulsed power generators using both an analytical equivalent circuit model and a SPICE simulation model. The new models of the capacitor were verified through frequency (1MHz to 50MHz) and time domain measurements. The measurements of the capacitor's behavior provided insight for the comparison between the analytical and SPICE models. The results were matched to the models representing the capacitor. In addition, placements of tabs, connecting to capacitor windings, were characterized to determine impact on the performance of the capacitor.

I. INTRODUCTION

This work is part of a SNL sponsored effort to evaluate the possibility of improving Linear Transformer Driver (LTD) performance by optimizing the design of the LTD cell capacitors. We began by determining the range of parameter variation possible in a basic 20 nF capacitor design. These capacitors can be constructed to either enhance their pulse line characteristics or to more closely approximate an ideal capacitor. By performing both frequency and time domain measurements on variously constructed 20 nF, 100 kV LTD capacitors we find their impedance characteristics and relate these to construction features. We then construct equivalent circuit models derived from analysis of these features and find good correlation between model and experiment.

A. Tests

Tests were done on special capacitors built for LTD testing. Two types of measurements were made. The first were driving point impedance measurements swept in the frequency domain from 1 MHz to 50 MHz. These measurements provide insight into the behavior of the capacitor compared to analytical and SPICE models. To verify models in the time domain, measurements were also made by using high voltage discharge of the capacitor into a resistive load.

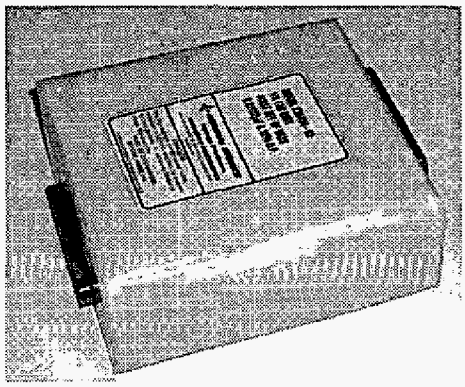

Figure 1. Capacitor for the LTD system.

B. Capacitor Construction

The physical extent of an energy storage capacitor will cause it to have distributed properties of wave impedance and transit time for the discharge of energy. These properties may be varied through construction variation while keeping capacitance fixed.

The LTD capacitor has multiple series connected windings in a plastic case with wide rail terminals on one end or opposite ends. The model 35404 units studied here are double ended units with a rail terminal on each end of an elongated rectangular case. Figure 1 is a photo of one of the LTD capacitors.

The capacitor is made of multiple series sections. Each section is made from rolled up foil and dielectric. Figure 2 shows an example prior to rolling.

* Sponsored by Sandia National Laboratories
ξ email: bushnell@ga-esi.com

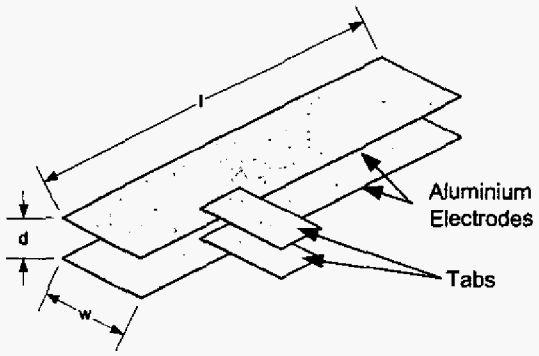

Figure 2 Unrolled capacitor pad construction.

This structure forms a strip line having terminals at the tabs. This connection puts two strip lines of impedance Z as in equation (1).

$$Z = \frac{120\pi}{\sqrt{\varepsilon_r}} \frac{d}{w} \tag{1}$$

The one way EM wave transit time for this is given in equation (2).

$$\delta = \frac{1 \cdot \sqrt{\varepsilon_r}}{2 \cdot c} \tag{2}$$

Tab position can be varied and more tabs cab be used. Note that the capacitance can be given by equation (3) and approximately doubles when this strip is wound up because both sides of the foil are used.

$$C = \frac{\varepsilon \cdot l \cdot w}{d} \tag{3}$$

Associated with this effect, the wave transit time along the length of the line doubles when the winding is rolled and flattened for packaging.

In this view one can see how construction contributes to inductance. Short circuiting the terminals produces a loop including the tabs which define a flux volume corresponding to inductance external to the winding.

Additional tabs inserted at other locations in the winding have the effect of placing the terminals nearer to the stored energy. Each pair of tabs reduces the source impedance and the transit time in the winding structure.

II. AC MEASUREMENTS

AC measurements were made using a waveform generator coupled to the test capacitor with a resistive network, which is shown in Figure 3. A photo of this network is shown in Figure 3. Measurement of the voltage on each side of the resistors allowed us to determine the voltage and current in the capacitor. From that we can calculate the complex driving point impedance of the capacitors. Voltage and frequency measurements were made with an Agilent 54825A oscilloscope. The use of an oscilloscope is important because it allows us to not only measure the voltage and phase angle but also to detect various forms of distortion.

Driving Point Impedance Calculations

At each frequency the RMS voltage out of the waveform generator, the RMS voltage across the capacitor and the phase angle between the voltages were measured. The RMS voltage measurements were made using an internal analysis tool in the oscilloscope. This tool removes any DC component from the measurement prior to the RMS calculations.

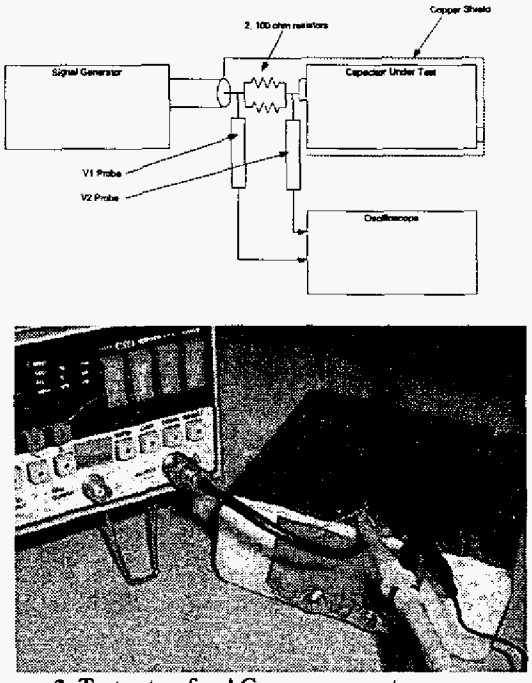

Figure 3. Test setup for AC measurements

The driving point impedance was calculated using the MATHCAD software package. This package allows complex numbers to be handled directly. V_1 is the voltage on the waveform generator and V_2 is the voltage on the capacitor. The first equation in (4-a) was used to calculate complex voltage for V_2. V_1 was assumed to have a phase angle of zero. The second equation in (4-b) was used to calculate the complex impedance vector.

$$V_{2_i} := V_{2_i} e^{-j \cdot angle_i \cdot \deg} \tag{4-a}$$

$$Z_i = \frac{50 \cdot \Omega}{\frac{V_{1_i}}{V_{2_i}} - 1} \tag{4-b}$$

An example of the data is shown in Figure 4. This plot shows the magnitude of the driving point impedance for a single tabbed capacitor.

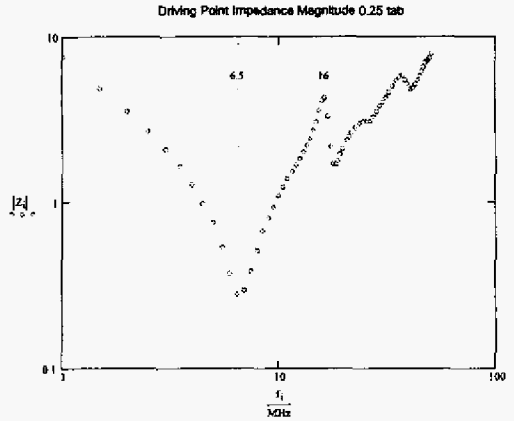

Figure 4. Driving point impedance of LTD capacitor with one tab at 0.25 point from start of winding.

III. AC DATA ANALYSIS AND MODELING

High voltage, high current film capacitors are manufactured by winding layers of foil and insulation. In the case of the LTD capacitors and many other type S plastic capacitors tabs are inserted during the winding process to allow connection to the foil. Figure 5 shows a diagram of a capacitor pad with a single tab pair inserted shown by the heavy diagonal lines.

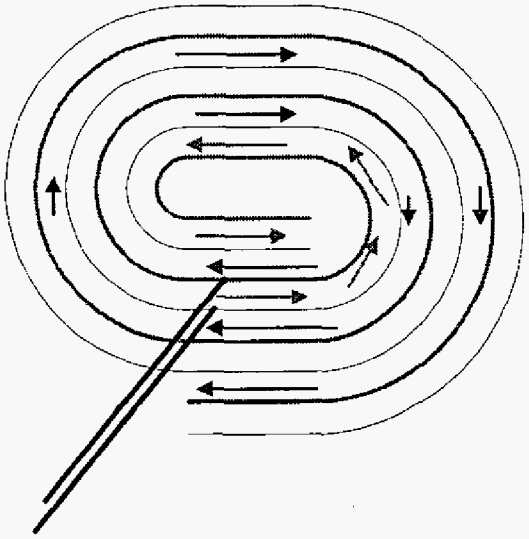

Figure 5. Wave propagation in capacitor winding

The strips of foil and dielectric wound in the capacitor pad form a transmission line structure. To trace the structure imagine a pulse launched into the transmission line structure at the black tabs. The wave launched will propagate both inward and outward in the capacitor structure. The red arrows represent the inward traveling wave. This wave spirals into the center of the capacitor (or the start in capacitor terms). After the pad is wound it is flattened and the opening in the center of the pad is minimized. This allows the inward propagating wave to travel outward toward the finish and is represented by the blue arrows in the diagram. This pulse will propagate all the way to the finish which forms an open circuit. A pulse also travels outward from the injection point to the finish of the winding and strikes the open circuit.

Figure 6 shows an equivalent circuit of the winding in Figure 5. The total transmission line length doubles when the pad is rolled up. The pair of transmission lines on the left represent the "front side" of the winding directly connected to the tabs. The single transmission line on the right represents the "back side" of the winding. An external inductance representing the tabs is added at the tap point of the transmission lines.

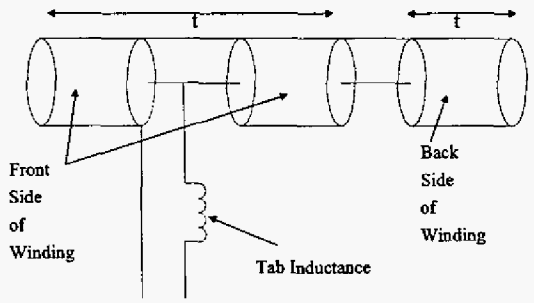

Figure 6. Equivalent circuit of a capacitor winding.

This circuit can be modeled analytically and numerically with the SPICE circuit code in the time and frequency domain.

IV. FREQUENCY DOMAIN MODEL

The driving point impedance of a single open circuit transmission line can be represented by equation (5).

$$Z(\varpi, d) := Z \cdot \frac{\left(1 + e^{-1 \cdot j \cdot \frac{\varpi}{v} \cdot d}\right)}{1 - e^{-1 \cdot j \cdot \frac{\varpi}{v} \cdot d}} \qquad (5)$$

Where, d is the length of the transmission line in meters, v is the propagation velocity in the transmission line, ω is the frequency in radians/sec and Z is the transmission line impedance.

This relation can be used by combining the two transmission lines in parallel and adding inductance and resistance in series with the transmission lines. This gives the relation (equations 6-a, 6-b) which is the frequency domain representation of the driving point impedance of the LTD capacitor.

$$Z_o := \frac{2 \cdot \tau}{C} \qquad (6\text{-a})$$

$$a := (1 - D) \cdot \tau \qquad \text{and} \qquad b := \tau + D \cdot \tau$$

$$Z_{cap}(\varpi) := \frac{Z_o}{2} \cdot \frac{\left(1 + e^{-2 \cdot i \cdot \varpi \cdot b}\right) \cdot \left(1 + e^{-2 \cdot i \cdot \varpi \cdot a}\right)}{1 - e^{-2 \cdot i \cdot \varpi \cdot (a+b)}}$$

$$+ \left(\varpi \cdot j \cdot L_b + R_{est}\right) \qquad \text{(6-b)}$$

Here, τ is the one way transit time of the winding before rolling, and D is the fraction of the winding were the tab is located from the start of the winding. By inspection, when the denominator of the equation goes to zero the impedance has a pole. The interesting feature of this pole is that the frequency of this pole is independent of D and only a function of the transmission line length. The frequency of the pole is given by equation (7).

$$f = \frac{n}{2 \cdot \tau} \qquad (7)$$

where n is a positive integer.

X35404 Modified 0.25 Tab AC data and model

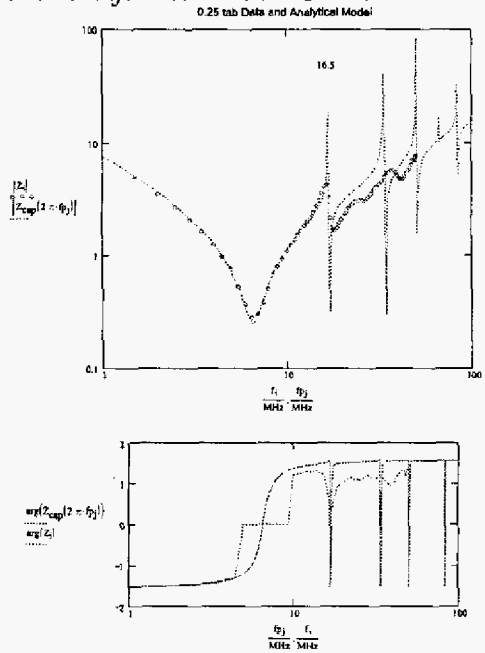

Figure 7. Comparison of analytical model and measured data for the 0.25 tab capacitor.

Figure 7 shows the measured impedance magnitude and phase and the prediction of the analytical model.

The 16.5 MHz pole corresponds to the pole from the denominator of the model. The first minimum corresponds to the normal LC resonance associated with the discrete RLC circuit. The graph below the driving point impedance is the phase angle of the driving point impedance for experimental data and the analytical model. The calculated magnitude and phase angle of the driving point impedance closely match the measured values.

V. TIME DOMAIN MEASUREMENTS

Time domain measurements are a direct functional determination of capacitor characteristics in a discharge circuit, which approximates conditions of use. Current or voltage waveforms were acquired for analysis to determine capacitor terminal inductance and equivalent series resistance (ESR). Other measurements used a resistive termination and current shunt to produce discharge current waveforms. Discharge measurements were made in the lowest inductance configuration with a close fitting ground return around the case to limit inductance to only that within the capacitor outline and associated with shunt probe connection and discharge switch. Discharge measurements were made at 5 to 10 kV using a low resistance solid dielectric switch.

Current shunt measurements of these are shown in Figures 8. Also included in this plot are data from SPICE calculations based on the analytical model. This shows the close match between the time domain and frequency domain models. The ½ tab position unit shows pronounced PFN like characteristics.

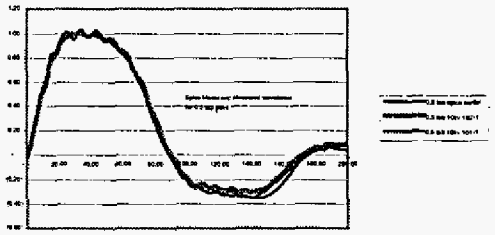

Figure 8. Comparison of a SPICE model and measured data for the 0.5 tab capacitor.

VI. CONCLUSION

The transmission line model has been demonstrated to accurately predict capacitor behavior. We are continuing to work on this problem by including frequency dependent parameters such as skin effect and losses driven by transmission line resonance.

REFERENCES

This paper has no references